

**Supporting Information**

---

**A *triangulo* palladium cluster consisting of  $\mu^3$ -capping silyl ligands**

Felix Armbruster<sup>a</sup>, Jens Meyer<sup>a</sup>, Alexander Baldes<sup>b</sup>, Pascual Oña Burgos<sup>a</sup>, Ignacio Fernández<sup>c</sup>, and Frank Breher<sup>a,\*</sup>

<sup>a</sup> Institute of Inorganic Chemistry, Karlsruhe Institute of Technology (KIT), Engesserstraße 15, 76131 Karlsruhe, Germany.

<sup>b</sup> Institute of Physical Chemistry, Karlsruhe Institute of Technology (KIT), Engesserstraße 15, 76131 Karlsruhe, Germany.

<sup>c</sup> Área de Química Orgánica, Universidad de Almería, Ctra. Sacramento s/n, 04120, Almeria, Spain

\* Author to whom correspondence should be addressed:

E-mail: breher@kit.edu

**Content:**

- General techniques.
- Details on the X-ray structure determination.
- Computational details.
- Experimental details: Preparation of **1** to **3**, NMR investigations on [*SP-4-2*]/[*SP-4-4*]-**4** and -**6**.
- Figure S1. Selected DFT calculated molecular orbitals of **3**.
- Results from our initial study on **3** to act as catalyst in a Suzuki-type cross-coupling reaction.
- Figure S2.  $^1\text{H}$ , $^{29}\text{Si}$  gHMQC spectrum of **3** at room temperature.
- Figure S3.  $^1\text{H}$ , $^{15}\text{N}$  gHMQC spectrum of **3** at room temperature.
- Figure S4.  $^1\text{H}$  NMR spectra as a function of temperature for  $[\text{PtH}(\text{P}t\text{Bu}_3)\{\text{Si}(\text{mt}^{\text{Me}})_3\}]$  (*[SP-4-2]*/*[SP-4-4]*-**6**).
- Figure S5.  $^1\text{H}$  NMR spectra as a function of temperature for  $[\text{PtH}(\text{P}t\text{Bu}_3)\{\text{Si}(\text{mt}^{\text{Me}})_3\}]$  (*[SP-4-2]*/*[SP-4-4]*-**6**) (olefinic region).
- Figure S6.  $^1\text{H}$  NMR spectra as a function of temperature for  $[\text{PtH}(\text{P}t\text{Bu}_3)\{\text{Si}(\text{mt}^{\text{Me}})_3\}]$  (*[SP-4-2]*/*[SP-4-4]*-**6**) (hydride region)
- Figure S7.  $^1\text{H}$  NMR spectrum for  $[\text{PtH}(\text{P}t\text{Bu}_3)\{\text{Si}(\text{mt}^{\text{Me}})_3\}]$  (*[SP-4-2]*/*[SP-4-4]*-**6**), showing couplings to  $^{31}\text{P}$  (100 %),  $^{195}\text{Pt}$  (ca. 30 %) and  $^{29}\text{Si}$  (4%).
- Figure S8.  $^1\text{H}$  NMR spectrum of the hydride region at 173 K showing the ratio between the two isomeric forms of  $[\text{PtH}(\text{P}t\text{Bu}_3)\{\text{Si}(\text{mt}^{\text{Me}})_3\}]$  (*[SP-4-2]*/*[SP-4-4]*-**6**).
- Figure S9.  $^1\text{H}$ , $^{29}\text{Si}$  gHMQC NMR spectrum of  $[\text{PtH}(\text{P}t\text{Bu}_3)\{\text{Si}(\text{mt}^{\text{Me}})_3\}]$  (*[SP-4-2]*/*[SP-4-4]*-**6**) at 173 K.
- Figure S10.  $^1\text{H}$ , $^{29}\text{Si}$  gHMQC NMR spectrum of  $[\text{PtH}(\text{P}t\text{Bu}_3)\{\text{Si}(\text{mt}^{\text{Me}})_3\}]$  (*[SP-4-2]*/*[SP-4-4]*-**6**) at 173 K (hydride region).
- Figure S11.  $^1\text{H}$ , $^{195}\text{Pt}$  gHMQC NMR spectrum of  $[\text{PtH}(\text{P}t\text{Bu}_3)\{\text{Si}(\text{mt}^{\text{Me}})_3\}]$  (*[SP-4-2]*/*[SP-4-4]*-**6**) at RT.
- Figure S12.  $^1\text{H}$ , $^{195}\text{Pt}$  gHMQC NMR spectrum of  $[\text{PtH}(\text{P}t\text{Bu}_3)\{\text{Si}(\text{mt}^{\text{Me}})_3\}]$  (*[SP-4-2]*/*[SP-4-4]*-**6**) at RT (hydride region).
- Figure S13.  $^1\text{H}$ , $^1\text{H}$  EXSY NMR spectrum of  $[\text{PtH}(\text{P}t\text{Bu}_3)\{\text{Si}(\text{mt}^{\text{Me}})_3\}]$  (*[SP-4-2]*/*[SP-4-4]*-**6**) at 193 K.
- Figure S14.  $^1\text{H}$ , $^1\text{H}$  EXSY NMR spectrum of  $[\text{PtH}(\text{P}t\text{Bu}_3)\{\text{Si}(\text{mt}^{\text{Me}})_3\}]$  (*[SP-4-2]*/*[SP-4-4]*-**6**) at 193 K (olefinic region).
- Figure S15.  $^1\text{H}$ , $^1\text{H}$  ROESY NMR spectrum of  $[\text{PtH}(\text{P}t\text{Bu}_3)\{\text{Si}(\text{mt}^{\text{Me}})_3\}]$  (*[SP-4-2]*/*[SP-4-4]*-**6**) at 173 K.
- Figure S16.  $^1\text{H}$ , $^1\text{H}$  ROESY NMR spectrum of  $[\text{PtH}(\text{P}t\text{Bu}_3)\{\text{Si}(\text{mt}^{\text{Me}})_3\}]$  (*[SP-4-2]*/*[SP-4-4]*-**6**) at 173 K (hydride region).
- Figure S17.  $^1\text{H}$ , $^1\text{H}$  ROESY NMR spectrum of  $[\text{PtH}(\text{P}t\text{Bu}_3)\{\text{Si}(\text{mt}^{\text{Me}})_3\}]$  (*[SP-4-2]*/*[SP-4-4]*-**6**) at 173 K (olefinic region).
- References of the Supporting Information.

## General techniques

All manipulations were performed under an argon atmosphere using standard Schlenk techniques. All solvents were freshly distilled under argon from sodium/benzophenone (THF), sodium-potassium alloy/tetraglyme/benzophenone (pentane, hexane),  $\text{CaSO}_4$  (acetone), or  $\text{CaH}_2$  (acetonitrile) and stored over molecular sieve (3 Å) (acetone, acetonitrile) prior to use.  $\text{D}_6\text{-dmso}$  was vacuum transferred from  $\text{CaCl}_2$  into thoroughly dried glassware equipped with Young teflon valves. Air sensitive compounds were stored and weighed in glove boxes (Braun MB150 G-I and Unilab system). Elemental analyses and mass spectroscopic analyses were carried out in the institutional technical laboratories. IR-spectra were measured using the ATR technique (attenuated total reflection) on a Bruker Vertex 70 spectrometer in the range from  $4000 \text{ cm}^{-1}$  to  $400 \text{ cm}^{-1}$ . The intensity of the absorption band is indicated as vw (very weak), w (weak), m (medium), s (strong), vs (very strong), and br (broad).

NMR spectra were measured on a Bruker Avance 400 spectrometer equipped with a third radiofrequency channel. A 5-mm indirect triple probe head was used. The outer coil was doubly tuned for  $^1\text{H}$  and  $^{31}\text{P}$ , and the inner coil was tuned for  $^{13}\text{C}$ ,  $^{29}\text{Si}$ ,  $^{31}\text{P}$ , and  $^{195}\text{Pt}$ . The spectral references used were TMS for  $^1\text{H}$ ,  $^{13}\text{C}$  and  $^{29}\text{Si}$ ,  $\text{H}_3\text{PO}_4$  (85%) for  $^{31}\text{P}$ , and  $\text{Na}_2\text{PtCl}_6$  for  $^{195}\text{Pt}$ . Coupling constants  $J$  are given in Hertz as positive values regardless of their real individual signs. The multiplicity of the signals is indicated as s, d, or m for singlets, doublets, or multiplets, respectively. NMR samples were always prepared in thoroughly dried 5-mm NMR tubes and sealed under argon or in vacuum. Unless otherwise stated, standard Bruker software routines (TOPSPIN and XWINNMR) were used for the 1D and 2D NMR measurements. Diffusion measurements were performed using the stimulated echo pulse sequence<sup>[S1]</sup> on a 400 MHz Bruker Avance spectrometer equipped with a

microprocessor controlled gradient unit and an inverse multinuclear probe with an actively shielded Z-gradient coil. The shape of the gradient pulse was rectangular, and its strength varied automatically in the course of the experiments. The  $D$  values were determined from the slope of the regression line  $\ln(I/I_0)$  versus  $G^2$ , according to the equation

$$\ln\left(\frac{I}{I_0}\right) = -(\gamma\delta)^2 G^2 \left(\Delta - \frac{\delta}{3}\right) D$$

$I/I_0$  = observed spin echo intensity/intensity without gradients,  $G$  = gradient strength,  $\Delta$  = delay between the midpoints of the gradients,  $D$  = diffusion coefficient,  $\delta$  = gradient length. The measurements were carried out without spinning. The calibration of the gradients was carried out via a diffusion measurement of HDO in D<sub>2</sub>O, which afforded a slope of  $1.99 \cdot 10^{-4}$ .<sup>[S2]</sup> We estimate the experimental error in the  $D$  values to be  $\pm 2\%$ . All of the data leading to the reported  $D$  values afforded lines whose correlation coefficients were  $> 0.999$  and 8-12 points have been used for regression analysis. To check reproducibility, three different measurements with different diffusion parameters ( $\delta$  and/or  $\Delta$ ) were always carried out. The gradient strength was incremented in 8% steps from 10% to 98%. A measurement of <sup>1</sup>H and  $T_1$  was carried out before each diffusion experiment, and the recovery delay set to 5 times  $T_1$ . In the diffusion experiments  $\delta$  was set to 3 ms, and the number of scans were 32-80 per increment with a recovery delay of 10 s. Typical experimental times were 2-4 h. The hydrodynamic radii  $r_H$  were calculated from the Stokes-Einstein equation,

$$D = (k_B T)/(6\pi\eta r)$$

in which  $D$  is the diffusion coefficient,  $k_B$  is the Boltzman constant,  $T$  is the temperature in Kelvin,  $\eta$  is the viscosity of the solvent, in this case DMSO ( $2.114 \times 10^{-3}$ ).<sup>[S3]</sup>

### X-ray structure determination

Red single crystals suitable for X-ray diffraction of **3** were obtained from a  $\text{CH}_2\text{Cl}_2$  solution at room temperature. In order to avoid quality degradation, the single crystals were mounted in perfluoropolyalkylether oil on top of a glass fiber and then brought into the cold nitrogen stream of a low-temperature device so that the oil solidified. Data collection for the X-ray structure determinations were performed on a STOE STADI 4 diffractometer with a CCD detector using graphite-monochromated  $\text{MoK}\alpha$  ( $0.71073 \text{ \AA}$ ) radiation and a low temperature device. The calculations were performed using SHELXTL (ver. 6.12) and SHELXL-97.<sup>[S4]</sup> The structure was solved by direct methods and successive interpretation of the difference Fourier maps, followed by full matrix least-squares refinement (against  $F^2$ ). The contribution of the hydrogen atoms, in their calculated positions, was included in the refinement using a riding model. Upon convergence, the final Fourier difference map of the X-ray structures showed only some residual electron density close to (disordered)  $\text{CH}_2\text{Cl}_2$  solvent molecules within the crystal lattice. Numerical absorption corrections did not furnish improved datasets. The molecule crystallise with four  $\text{CH}_2\text{Cl}_2$  molecules as indicated by the formula  $\text{C}_{24}\text{H}_{30}\text{N}_{12}\text{Pd}_3\text{S}_6\text{Si}_2 \cdot 4(\text{CH}_2\text{Cl}_2)$ . One methylene chloride solvent molecules were seen to have abnormally large displacement parameters, indicative of disorder. This molecule was modelled as being disordered over two positions (FVAR = 0.75 in SHELXL). The coordinates, anisotropic displacement parameters and site occupancies of the disordered C and Cl atoms were refined to

loose restraints on the associated distances and displacement parameters. The SHELXL instruction ISOR was used for the disordered C and Cl atoms.

Selected distances ( $\text{\AA}$ ) and angles ( $^\circ$ ): Pd1–Pd2 2.7268(9), Pd1–Pd3 2.7188(8), Pd2–Pd3 2.7476(8), Pd1–Si1 2.411(2), Pd2–Si1 2.395(2), Pd3–Si1 2.382(2), Pd1–Si2 2.409(2), Pd2–Si2 2.380(2), Pd3–Si2 2.406(2), Pd1–S3 2.383(2), Pd1–S6 2.395(2), Pd2–S2 2.380(2), Pd2–S4 2.379(2), Pd3–S1 2.388(2), Pd3–S5 2.381(2), Si1···Si2 3.610; Pd1–Si1–Pd2 69.14(5), Pd1–Si1–Pd3 69.13(5), Pd2–Si1–Pd3 70.23(5), Pd1–Si2–Pd2 69.41(5), Pd1–Si2–Pd3 68.75(5), Pd2–Si2–Pd3 70.07(5).

## Computational details

All calculations were carried out with an up to date version of the TURBOMOLE program package.<sup>[S5]</sup> The geometries were optimized under exploitation of symmetry at DFT level using the BP86 functional<sup>[S6]</sup> and def2-TZVP basis sets<sup>[S7]</sup> for all atoms. For the RI-approximation the respective auxiliary basis sets were used.<sup>[S8]</sup> Natural population analysis<sup>[S9]</sup> (NPA) and population analysis based on occupation numbers<sup>[S10]</sup> (PABOON) were used as implemented in TURBOMOLE.

## Preparative details

*Preparation of Me<sub>3</sub>Si(mt<sup>Me</sup>) (1) (mt<sup>Me</sup> = 3-methylimidazoline-2-thione):*

To a stirred solution of Me<sub>3</sub>SiCl (9.7 mL, 75.7 mmol) in 20 mL THF a suspension of NaH (1.920 g, 80.0 mmol) and 2-mercaptop-1-methylimidazole (8.643 g, 75.7 mmol) in 60 mL THF was slowly added over a glass frit. After being stirred for 1h, the solvent was removed *in vacuo* following addition of 60 mL toluene. The product was isolated by filtration, dried *in vacuo* yielding a colourless oil, which crystallises after shock-freezing in liquid nitrogen to give a colourless solid. Yield 10.55 g, 75%.

<sup>1</sup>H NMR (C<sub>6</sub>D<sub>6</sub>):  $\delta$  0.45 (s, 9 H, Me<sub>Si</sub>), 3.04 (s, 3 H, Me<sub>im</sub>), 5.98 (d, 2 H, CH<sub>im</sub>), 5.80 (d, 2 H, CH<sub>im</sub>).

<sup>13</sup>C{<sup>1</sup>H} NMR:  $\delta$  0.09 (s, 3 C, Me<sub>Si</sub>, <sup>1</sup>J(<sup>13</sup>C, <sup>29</sup>Si) = 59.4 Hz), 34.6 (s, 1 C, Me<sub>im</sub>), 117.5 (s, 1 C, CH<sub>im</sub>), 119.9 (s, 1 C, CH<sub>im</sub>), 170.6 (s, 1 C, C=S).

<sup>29</sup>Si NMR (ineptnd):  $\delta$  14.3 (s).

Elemental analysis (%): Calcd. for C<sub>7</sub>H<sub>14</sub>N<sub>2</sub>SSi [186.06] (Found): C 45.12 (45.31), H 7.57 (7.84), N 15.03 (14.89), Si 15.07.

EI-MS m/z (%): 186 (100) [Me<sub>3</sub>Si(mt<sup>Me</sup>)]<sup>+</sup>, 171 (76.48) [Me<sub>2</sub>Si(mt<sup>Me</sup>)]<sup>+</sup>, 113 (27.78) [mt<sup>Me</sup>]<sup>+</sup>, 73 (94.22) [Me<sub>3</sub>Si]<sup>+</sup>.

IR (ATR, cm<sup>-1</sup>): 467 (m), 546 (s), 602 (vw), 633 (m), 665 (s), 708 (m), 728 (w), 764 (s), 839 (vs, br), 989 (m), 1028 (w), 1088 (m), 1138 (m), 1174 (s), 1242 (vs), 1265 (w), 1364 (vs), 1400 (m), 1451 (s), 1574 (m), 2897 (br), 2949 (w), 2976 (w), 3016 (br), 3107 (br), 3131 (w), 3158 (w).

*Preparation of HSi(mt<sup>Me</sup>)<sub>3</sub> (2H):*

HSiCl<sub>3</sub> (0.2 mL, 2 mmol) and 3 equivs. of **1** (1.116 g, 6 mmol) were placed in a Schlenk tube and 20 mL of toluene was added. The reaction mixture was stirred in a closed reaction vessel for 12h at 70°C yielding a colourless, loose solid. The material

was isolated by filtration and washed twice with 10 mL of toluene and 20 mL hexane. Finally, the colourless powder was dried *in vacuo* for 4 h at RT. Yield: 596 mg, 81%. M.p. (sealed tube under argon) >260°C (decomp).

<sup>1</sup>H NMR (CD<sub>3</sub>CN): (only hardly soluble) δ 3.52 (s, 9 H, Me), 6.50 (d, 3 H, CH, <sup>1</sup>J(<sup>1</sup>H,<sup>1</sup>H) = 2.44 Hz), 6.95 (d, 6 H, CH, <sup>1</sup>J(<sup>1</sup>H,<sup>1</sup>H) = 2.44 Hz). Some further signals which belong to impurities and/or decomposition products are also visible.

Elemental analysis (%): Calcd. for C<sub>12</sub>H<sub>16</sub>N<sub>6</sub>S<sub>3</sub>Si [386.58] (Found): C 39.10 (39.02), H 4.38 (4.70), N 22.80 (22.70).

EI-MS m/z (%): 367.9 (75.01) [HSi(mt<sup>Me</sup>)<sub>3</sub>], 254.8 (94.51) [HSi(mt<sup>Me</sup>)<sub>2</sub>]<sup>+</sup>, 140.9 (100) [HSi(mt<sup>Me</sup>)]<sup>2+</sup>.

IR (ATR, cm<sup>-1</sup>): 410 (w), 440 (m), 483 (w), 493 (m), 530 (w), 581 (s), 600 (w), 678 (s), 715 (w), 735 (vs), 765 (vs), 828 (br), 862 (w), 999 (w), 1033 (w), 1093 (w), 1133 (m), 1190 (vs), 1257 (s), 1297 (vw), 1371 (vs), 1398 (w), 1458 (s), 1575 (m), 1706 (vw), 2322 (w), 2935 (br), 3026 (br), 3098 (m), 3120 (w), 3160 (w).

*Preparation of [Pd<sub>3</sub>{Si(mt<sup>Me</sup>)<sub>3</sub>}<sub>2</sub>] (3):*

3 equivs. of [Pd(PtBu<sub>3</sub>)<sub>2</sub>] (409 mg, 0.8 mmol) and 2 equivs. of **2H** (530 mg, 0.53 mmol) were placed in a Schlenk tube and 30 mL of CH<sub>2</sub>Cl<sub>2</sub> was added. The reaction mixture was stirred for ca. 2 minutes yielding a clear yellow solution. Stirring was stopped and the reaction vessel was kept at room temperature over night. Orange-red crystals precipitated from the orange-red solution, which subsequently were isolated by filtration and washed twice with 10 mL hexane. Yield: 152 mg, 56%. M.p. (sealed tube under argon) >170°C (decomp.).

<sup>1</sup>H NMR (D<sub>8</sub>-dmso): δ 3.48 (s, 18 H, Me), 5.26 (d, 6 H, C<sub>5</sub>-H, <sup>1</sup>J(<sup>1</sup>H,<sup>1</sup>H) = 2.9 Hz), 7.13 (d, 6 H, C<sub>4</sub>-H, <sup>1</sup>J(<sup>1</sup>H,<sup>1</sup>H) = 2.9 Hz).

$^{13}\text{C}\{\text{H}\}$  NMR:  $\delta$  34.4 (s, 6 C, Me<sub>im</sub>), 118.3 (s, 6 C, C<sub>5</sub>), 123.7 (s, 6 C, C<sub>4</sub>), 163.5 (s, 6 C, CS).

$^{29}\text{Si}$  NMR (indirect detection gHMQC):  $\delta$  0.65

Elemental analysis (%): Calcd. for C<sub>24</sub>H<sub>30</sub>N<sub>12</sub>Pd<sub>3</sub>S<sub>6</sub>Si<sub>2</sub> [1054.40] (Found): C 27.34 (27.35), H 2.87 (2.90), N 15.94 (15.30).

IR (ATR, cm<sup>-1</sup>): 415 (w), 455 (w), 515 (vs), 582 (m), 594 (m), 621 (w), 692 (vs), 732 (m), 744 (s), 779 (w), 799 (vw), 831 (w), 969 (m), 1001 (w), 1028 (m), 1123 (s), 1143 (m), 1190 (w), 1300 (s), 1336 (w), 1380 (w), 1416 (w), 1431 (s), 1455 (w), 1483 (m), 1546 (s), 2862 (w), 2921 (w), 3024 (w), 3056 (m), 3127 (w).

ESI-MS: 1053.77 [Pd<sub>3</sub>{Si(mt<sup>Me</sup>)<sub>3</sub>}<sub>2</sub>]<sup>+</sup>

*<sup>1</sup>H NMR spectroscopic investigations on [PdH(PtBu<sub>3</sub>)<sub>2</sub>{Si(mt<sup>Me</sup>)<sub>3</sub>} ([SP-4-2]/[SP-4-4]-4)*

Pd(PtBu<sub>3</sub>)<sub>2</sub> (26 mg, 0.05 mmol) and 2 equivs. of **2H** (37 mg, 0.1 mmol) were placed in an NMR tube and 0.6 mL of CD<sub>2</sub>Cl<sub>2</sub> was added at -196°C and sealed under vacuum. The sample was monitored by <sup>1</sup>H NMR right after unfreezing of the solvent. The appearance of a small signal in the high field region at -6.35 ppm suggested the forming of a species consisting of a Pd–H bond. After 30 minutes, this signal disappeared and the precipitation of an orange solid indicated the formation of **3**. This observation was further supported by a simultaneous appearance and disappearance of dissolved H<sub>2</sub> ( $\delta$  4.63 ppm) in the <sup>1</sup>H NMR.

*NMR spectroscopic investigations on [PtH(PtBu<sub>3</sub>)<sub>2</sub>{Si(mt<sup>Me</sup>)<sub>3</sub>} ([SP-4-2]/[SP-4-4]-6)*

[Pt(PtBu<sub>3</sub>)<sub>2</sub>] (60 mg, 0.1 mmol) and **2** (37 mg, 0.1 mmol) were placed in an NMR tube and 0.6 mL of CD<sub>2</sub>Cl<sub>2</sub> was added. After approximately 2h, the yellowish solution became colourless. The reaction progress was monitored by <sup>1</sup>H and <sup>31</sup>P NMR

spectroscopy. Already after few minutes, a small signal at –9.55 ppm  $\{{}^1J({}^1H, {}^{195}Pt) = 1156.8 \text{ Hz}\}$  could be detected in the  ${}^1H$  NMR indicating the formation of a species consisting of a Pt–H moiety. The complete conversion was confirmed by disappearance of the  ${}^{31}P$  signal of the starting material  $[Pd(Pt-Bu_3)_2]$  {100.3 ppm,  ${}^1J({}^{31}P, {}^{195}Pt) = 4413 \text{ Hz}\}$ .

${}^1H$  NMR ( $CD_2Cl_2$ ):  $\delta$  –9.73 (d, 1 H, Pt–H,  ${}^1J({}^1H, {}^{195}Pt) = 1140.1 \text{ Hz}$ ,  ${}^2J({}^1H, {}^{29}Si) = 8.3 \text{ Hz}$ ,  ${}^2J({}^1H, {}^{31}P) = 16.4 \text{ Hz}$ ), 1.54 (d, 18 H,  $Me_{t-Bu}$ ,  ${}^3J({}^1H, {}^{31}P) = 12.0 \text{ Hz}$ ), 3.54 (s, 18 H,  $Me_{im}$ ,  ${}^1J({}^1H, {}^{13}C) = 140.5 \text{ Hz}$ ), 6.83 (s, 6 H,  $C_4-H_{im}$ ), 7.46 (bs, 6 H,  $C_5-H_{im}$ ).

${}^{13}C\{{}^1H\}$  NMR:  $\delta$  32.4 (d, 9 C,  $Me_{t-Bu}$ ,  ${}^2J({}^{13}C, {}^{31}P) = 4.6 \text{ Hz}$ ), 34.4 (s, 3 C,  $Me_{im}$ ,  ${}^4J({}^{13}C, {}^{195}Pt) = 2.4 \text{ Hz}$ ), 39.6 (d, 1C,  $C_{t-Bu}$ ,  ${}^1J({}^{13}C, {}^{31}P) = 9.1 \text{ Hz}$ ,  ${}^2J({}^{13}C, {}^{195}Pt) = 20.5 \text{ Hz}$ ), 120.3 (s, 3 C,  $C_4$ ), 121.8 (s, 3 C,  $C_5$ ,  ${}^3J({}^{13}C, {}^{195}Pt) = 27.7 \text{ Hz}$ ), 167.5 (d, 3 C, C=S,  ${}^3J({}^{13}C, {}^{31}P) = 4.3 \text{ Hz}$ ).

${}^{29}Si$  NMR (178K, indirect detection HMQC):  $\delta$  –220.1 (s, 1 Si, [SP-4-4]-isomer,  ${}^1J({}^{29}Si, {}^{195}Pt) = 243.0 \text{ Hz}$ ), –216.1 (s, 1 Si, [SP-4-2]-isomer).

${}^{31}P\{{}^1H\}$  NMR:  $\delta$  94.1 (s, 1 P,  ${}^1J({}^{31}P, {}^{195}Pt) = 2192.5 \text{ Hz}$ ).

${}^{195}Pt$  NMR (RT, indirect detection HMQC):  $\delta$  –6331.9 (d, 1 Pt, [SP-4-4]-isomer,  ${}^1J({}^{31}P, {}^{195}Pt) = 2192.5 \text{ Hz}$ ,  ${}^1J({}^{29}Si, {}^{195}Pt) = 248.0 \text{ Hz}$ ), –6348.4 (d, 1 Pt, [SP-4-2]-isomer,  ${}^1J({}^{195}Pt, {}^{31}P) = 2154.7 \text{ Hz}$ ).

${}^{195}Pt$  NMR (178K, indirect detection HMQC):  $\delta$  –6333.1 (d, 1 Pt, [SP-4-4]-isomer,  ${}^1J({}^{31}P, {}^{195}Pt) = 2192.5 \text{ Hz}$ ,  ${}^1J({}^{29}Si, {}^{195}Pt) = 243.0 \text{ Hz}$ ), –6348.4 (d, 1 Pt, [SP-4-2]-isomer,  ${}^1J({}^{195}Pt, {}^{31}P) = 2154.7 \text{ Hz}$ ).

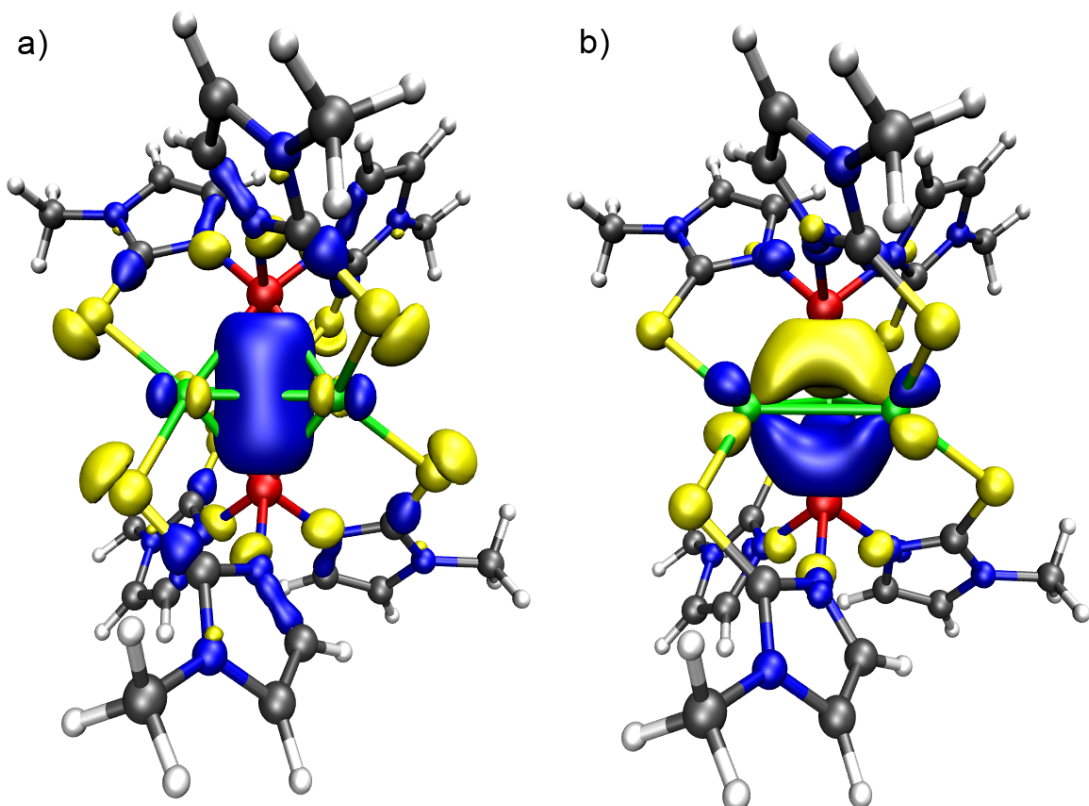
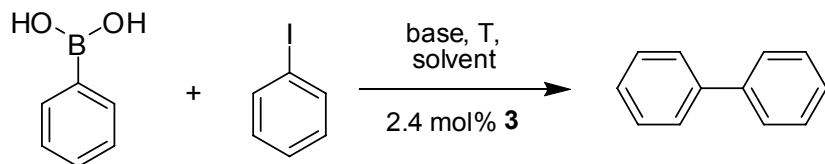


Figure S1. Selected DFT calculated molecular orbitals involved in the bonding of the  $\mu^3$ -capping  $\text{SiR}_3$  donors (red) with the palladium triangle (green): a)  $32a_1$ ; b)  $32a_2$ . NPA and PABOON results: Si: +0.239, +1.291; Pd: -0.010, +0.103; S: -0.334, -0.184.

## Catalytic studies

Initial studies towards a potential catalytic activity of **3** have been carried out using typical Suzuki-Miyaura-type cross-coupling conditions. Phenyl boronic acid and phenyl iodide have been employed as model reactants (Scheme S1). The parameters evaluated have been: a) base ( $\text{K}_2\text{CO}_3$ ,  $\text{Na}_2\text{CO}_3$  and  $\text{Et}_3\text{N}$ ); b) solvent (DMSO, DMF); temperature.



Scheme S1. General conditions.

In each case we have used catalyst loading of 2.4 mol% **3**. The conversion was checked by  $^{13}\text{C}$  NMR and GC-MS. The solvent of choice was DMSO in which **3** is soluble and stable. By contrast, **3** is only hardly soluble at room temperature in DMF. However, as can be seen from entry 5 in Table S1, we obtained similar results as compared to those in DMSO. A detailed study on the catalytic properties of **3** will be published elsewhere.

Table S1. Results

Entry	Solvent	Base		T (°C)	t (h)	Conversion
		type	equiv.			
1	DMSO	$\text{K}_2\text{CO}_3$	2	100	36	60
2	DMSO	$\text{K}_2\text{CO}_3$	2	140	12	85
3	DMSO	$\text{Na}_2\text{CO}_3$	2	100	36	55
4	DMSO	$\text{Et}_3\text{N}$	5	100	7	> 97
5	DMF	$\text{Et}_3\text{N}$	5	100	7	> 97

### NMR spectra (Figures S2 to S17)

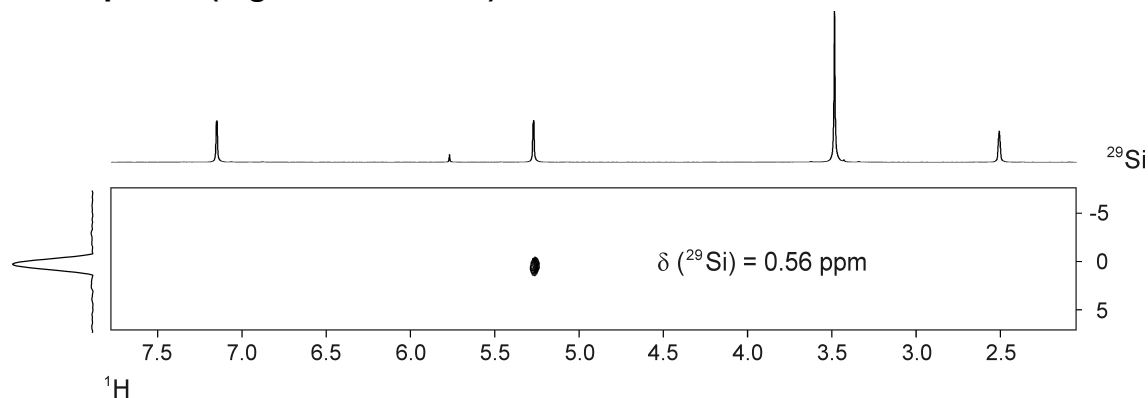


Figure S2.  $^1\text{H}, ^{29}\text{Si}$  gHMQC spectrum of **3** at room temperature.

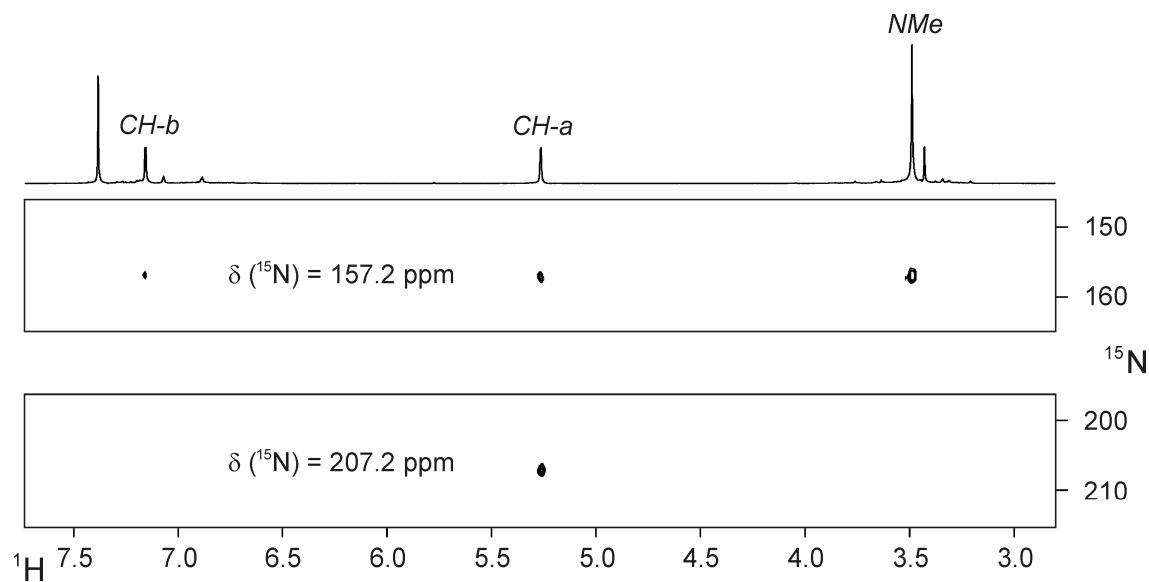


Figure S3.  $^1\text{H}, ^{15}\text{N}$  gHMQC spectrum of **3** at room temperature.

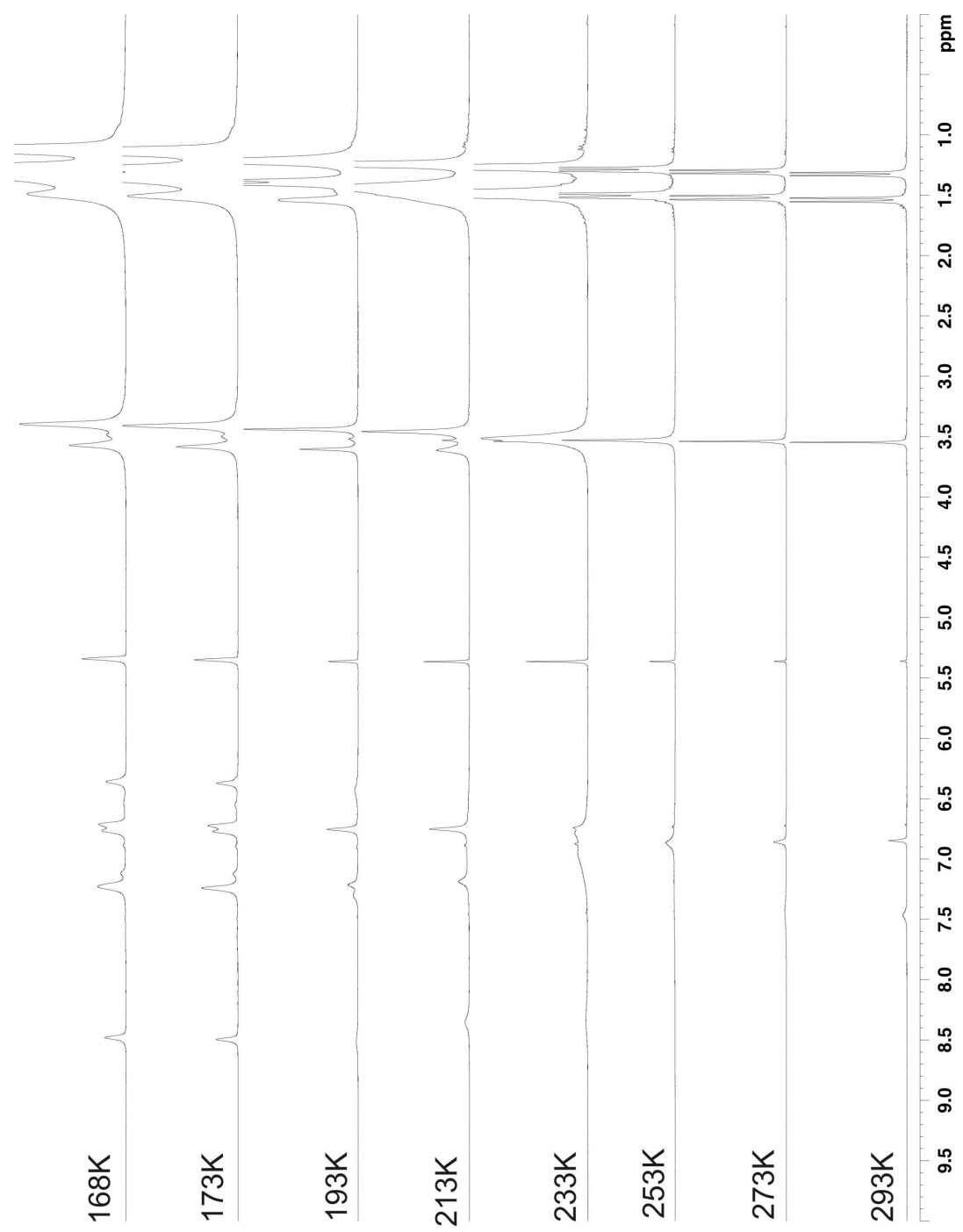


Figure S4. <sup>1</sup>H NMR spectra as a function of temperature for [PtH(PtBu<sub>3</sub>)<sub>2</sub>Si(mt<sup>Me</sup>)<sub>3</sub>] ([SP-4-2]/[SP-4-4]-6)

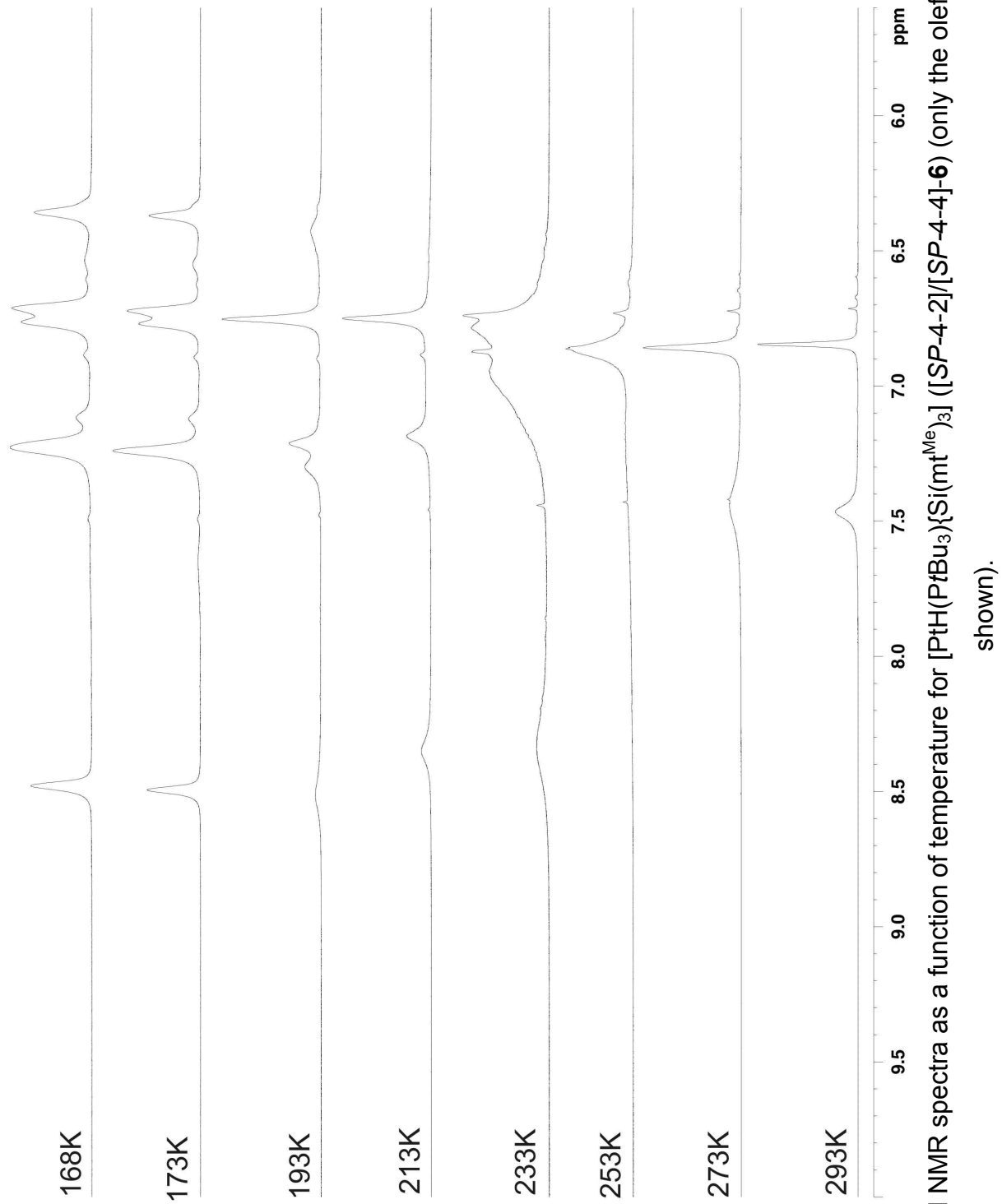


Figure S5.  $^1\text{H}$  NMR spectra as a function of temperature for  $[\text{PtH}(\text{P}t\text{Bu}_3)\{\text{Si}(\text{mt}^{\text{Me}})_3\}][\text{SP-4-2}]/[\text{SP-4-4}]\text{-6}$  (only the olefinic region is shown).

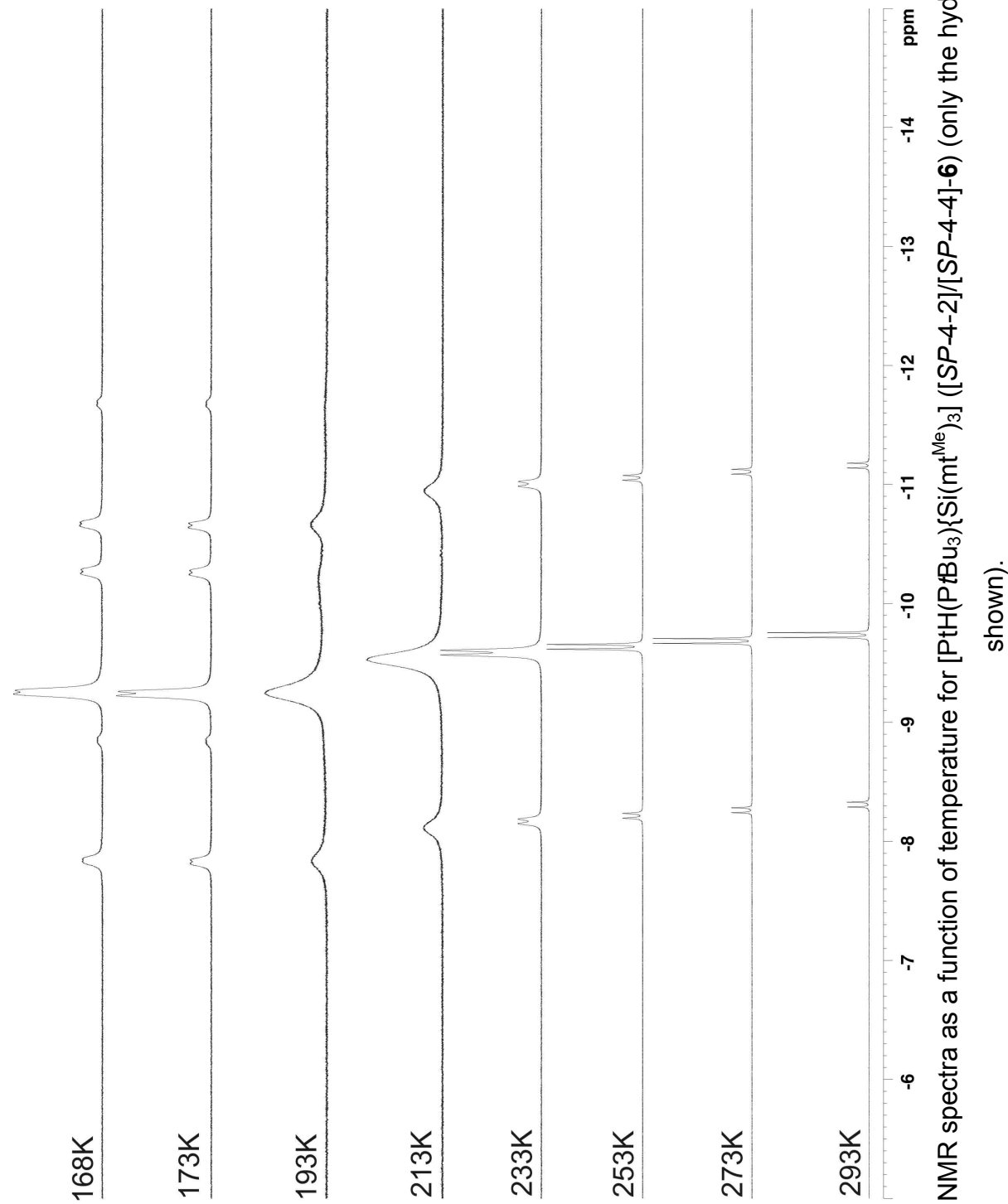


Figure S6.  $^1\text{H}$  NMR spectra as a function of temperature for  $[\text{PtH}(\text{P}t\text{Bu}_3)\{\text{Si}(\text{mt}^{\text{Me}})_3\}][\text{SP}-4-2]/[\text{SP}-4-4]-\mathbf{6}$  (only the hydride region is shown).

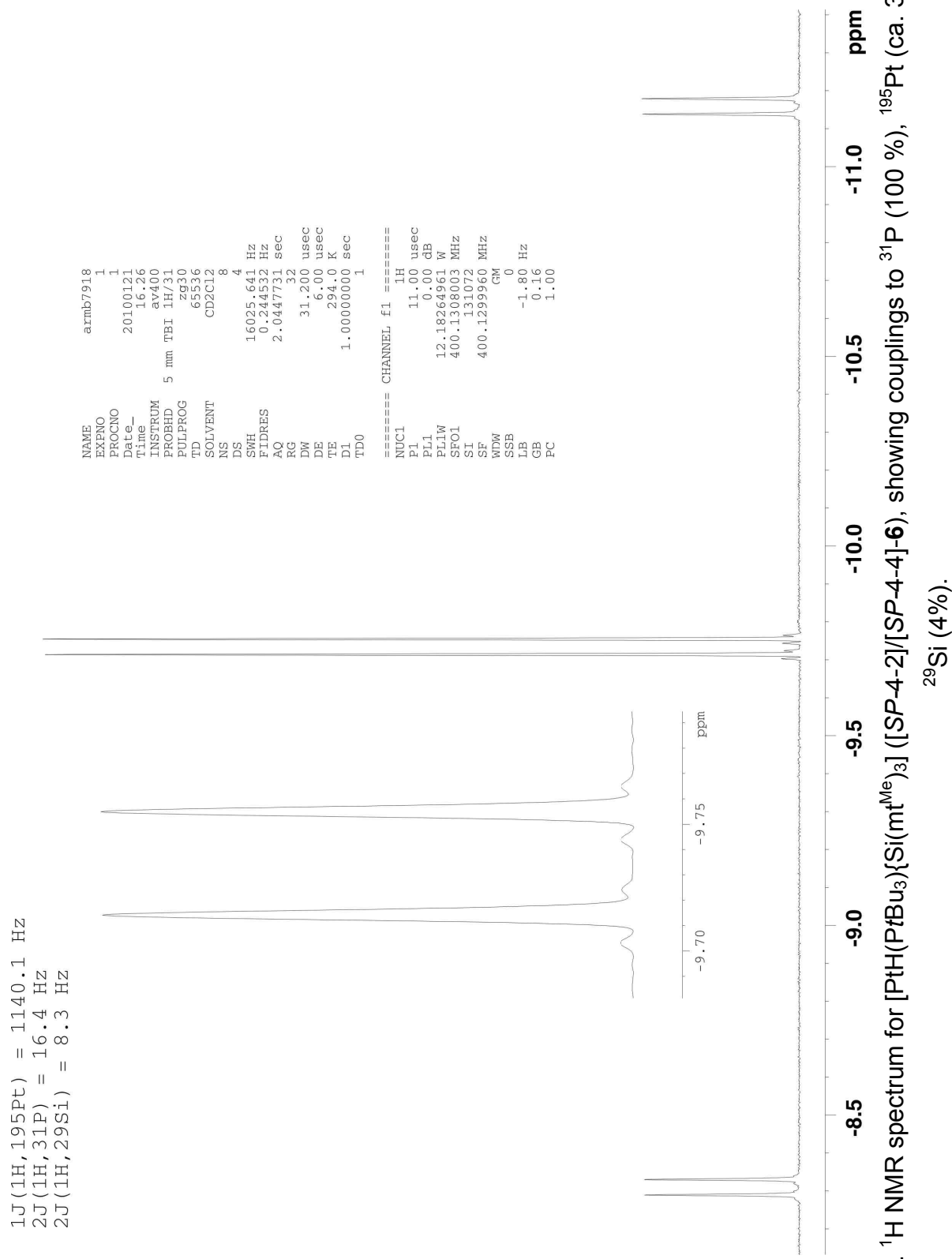


Figure S7.  ${}^1\text{H}$  NMR spectrum for  $[\text{PtH}(\text{PtBu}_3)\{\text{Si}(\text{mt}^{\text{Me}})_3\}][\text{SP4-2}]/[\text{SP4-6}]$ , showing couplings to  ${}^{31}\text{P}$  (100 %),  ${}^{195}\text{Pt}$  (ca. 30 %) and  ${}^{29}\text{Si}$  (4 %).

ratio of  $[SP\text{-}4\text{-}4]/[SP\text{-}4\text{-}2]$ -isomer  
is about 4:1

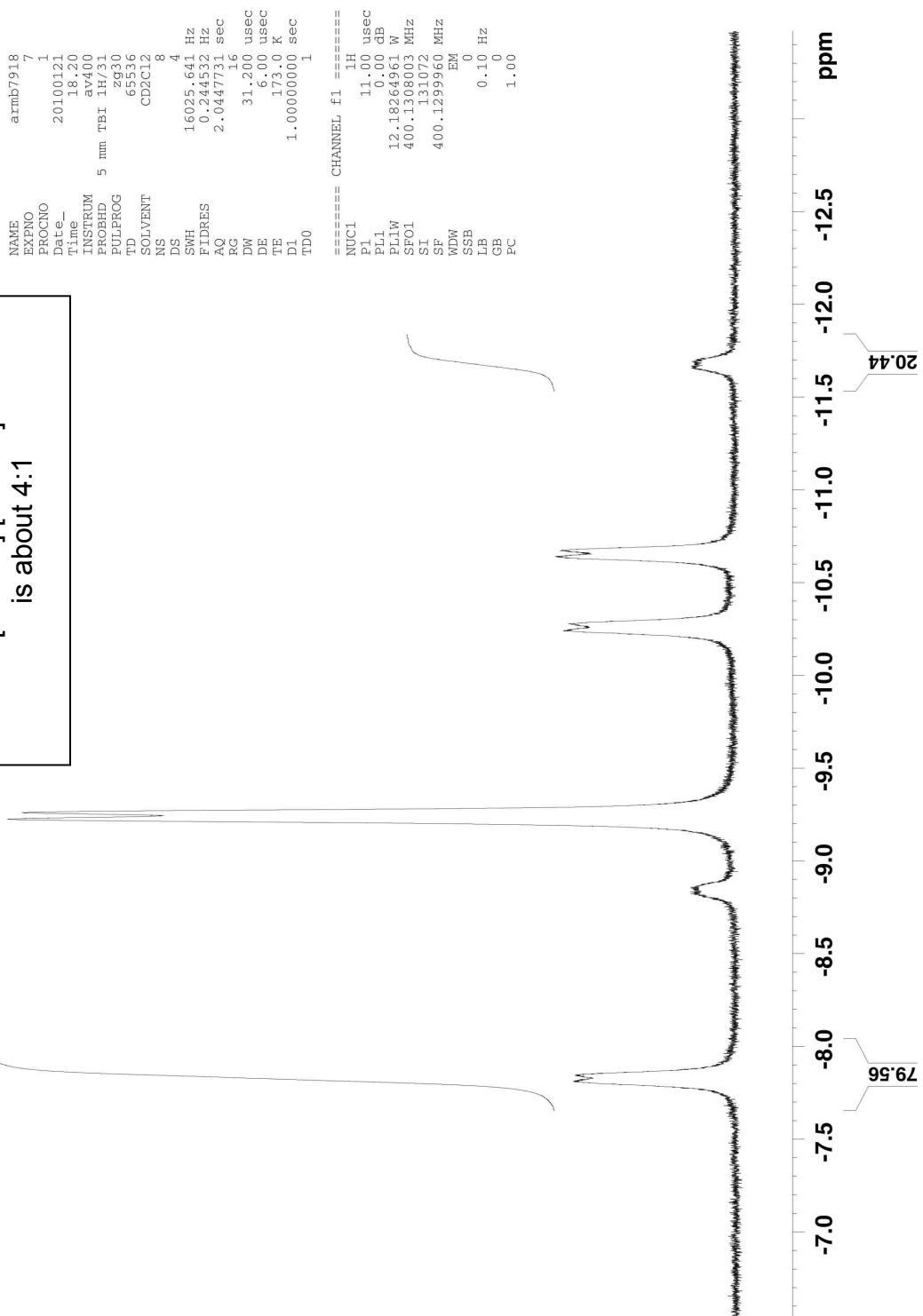


Figure S8.  $^1\text{H}$  NMR spectrum of the hydride region at 173 K showing the ratio between the two isomeric forms of  $[\text{PtH}(\text{PtBu}_3)\{\text{Si}(\text{mt}^{\text{Me}})_3\} ([\text{SP}\text{-}4\text{-}2]/[\text{SP}\text{-}4\text{-}4]\text{-}6)$ .

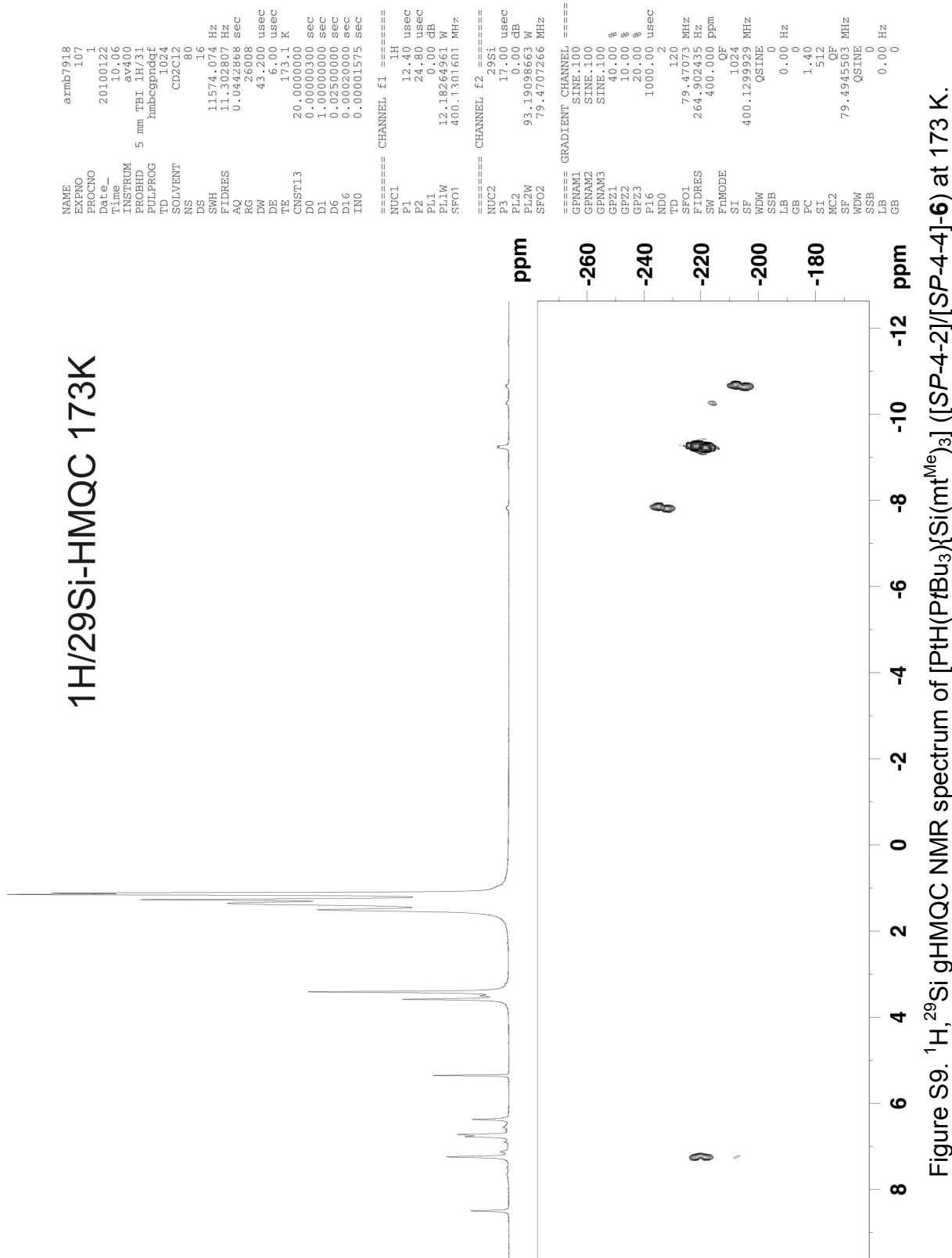


Figure S9.  $^1\text{H}$ ,  $^{29}\text{Si}$  gHMQC NMR spectrum of  $[\text{PtH}(\text{PtBu}_3)\{\text{Si}(\text{mt}^{\text{Me}})\}_3]$  ( $[\text{SP-4-2}][\text{SP-4-4-6}]$ ) at 173 K.

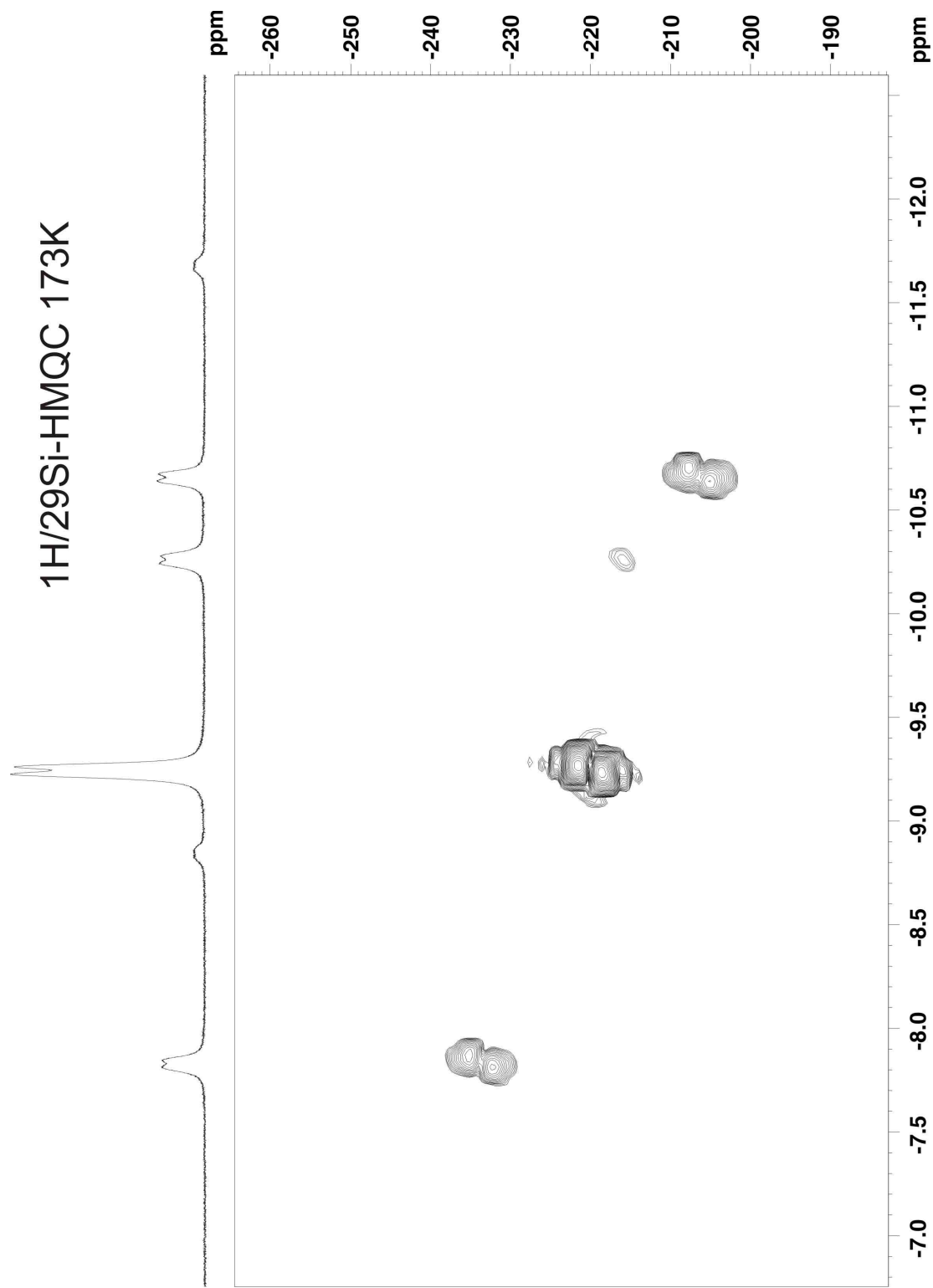


Figure S10.  $^1\text{H}$ ,  $^{29}\text{Si}$  gHMQC NMR spectrum of  $[\text{PtH}(\text{P}t\text{Bu}_3)\{\text{Si}(\text{mt}^{\text{Me}})_3\}]$  ( $[\text{SP-4-2}]/[\text{SP-4-4-6}]$ ) at 173 K (only the hydride region is shown).

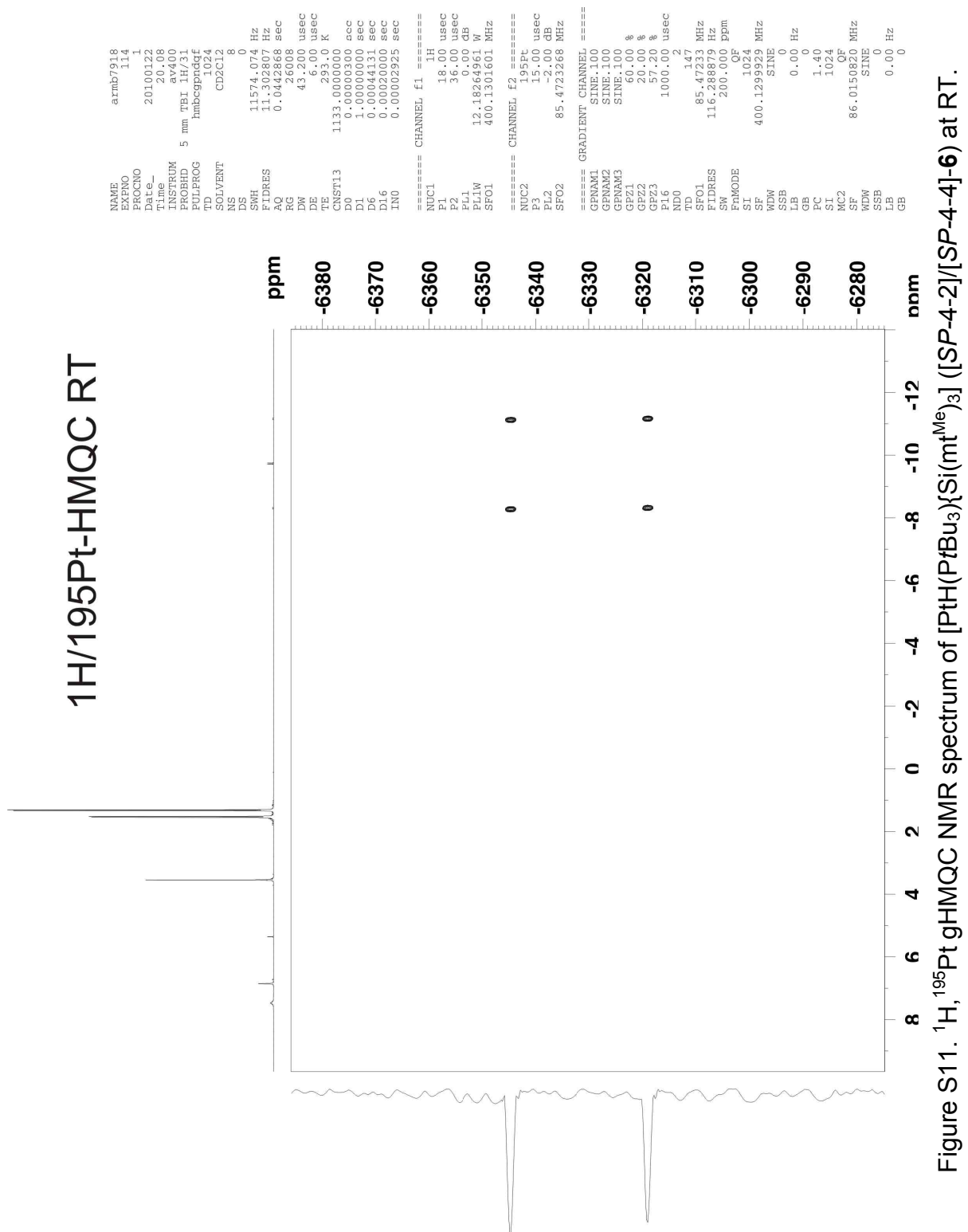


Figure S11.  $^1\text{H}$ ,  $^{195}\text{Pt}$  gHMQC NMR spectrum of  $[\text{PtH}(\text{PtBu}_3)\{\text{Si}(\text{mt}^{\text{Me}})_3\} ([\text{SP-4-2}]/[\text{SP-4-4}]\text{-6})$  at RT.

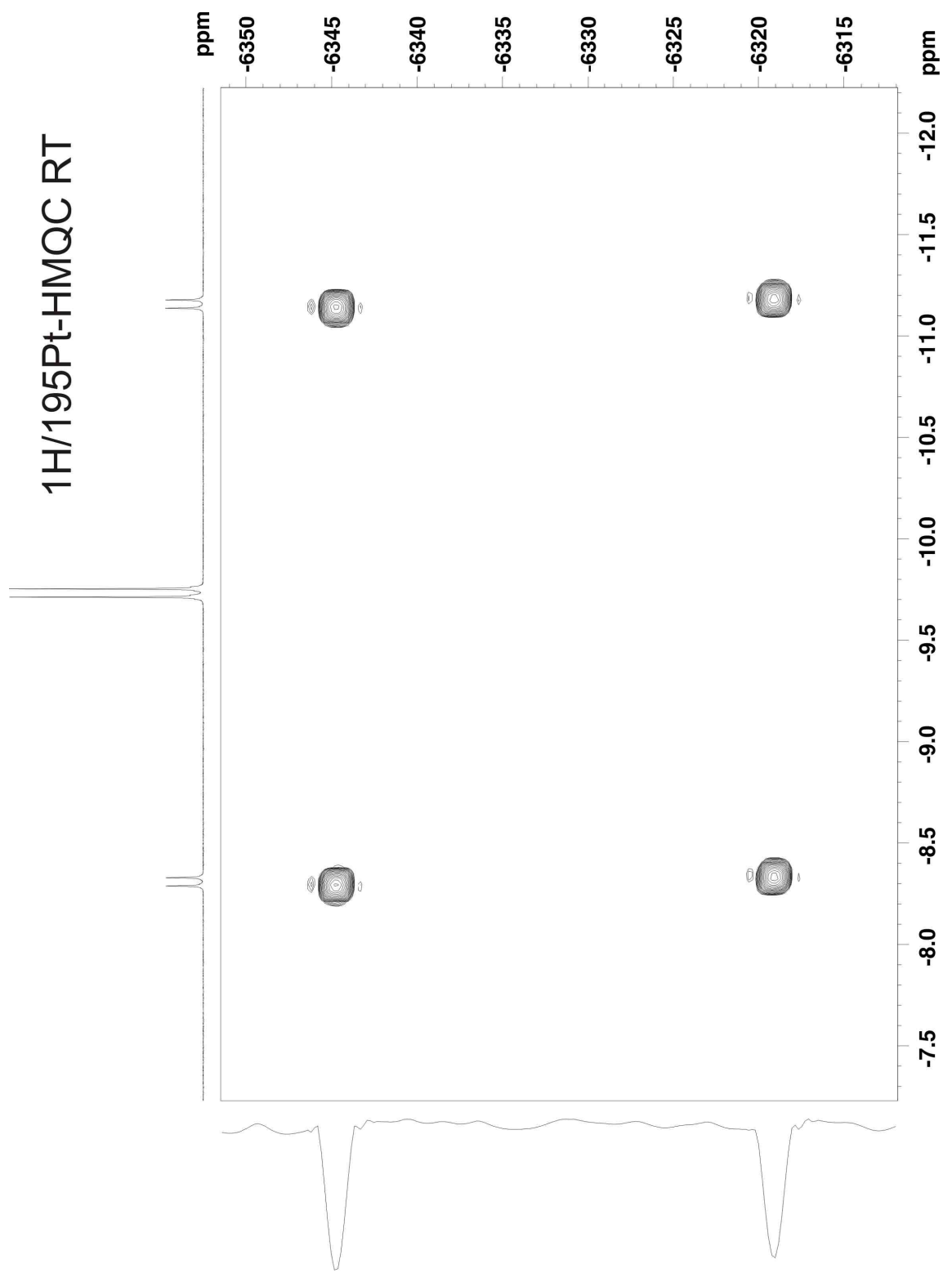
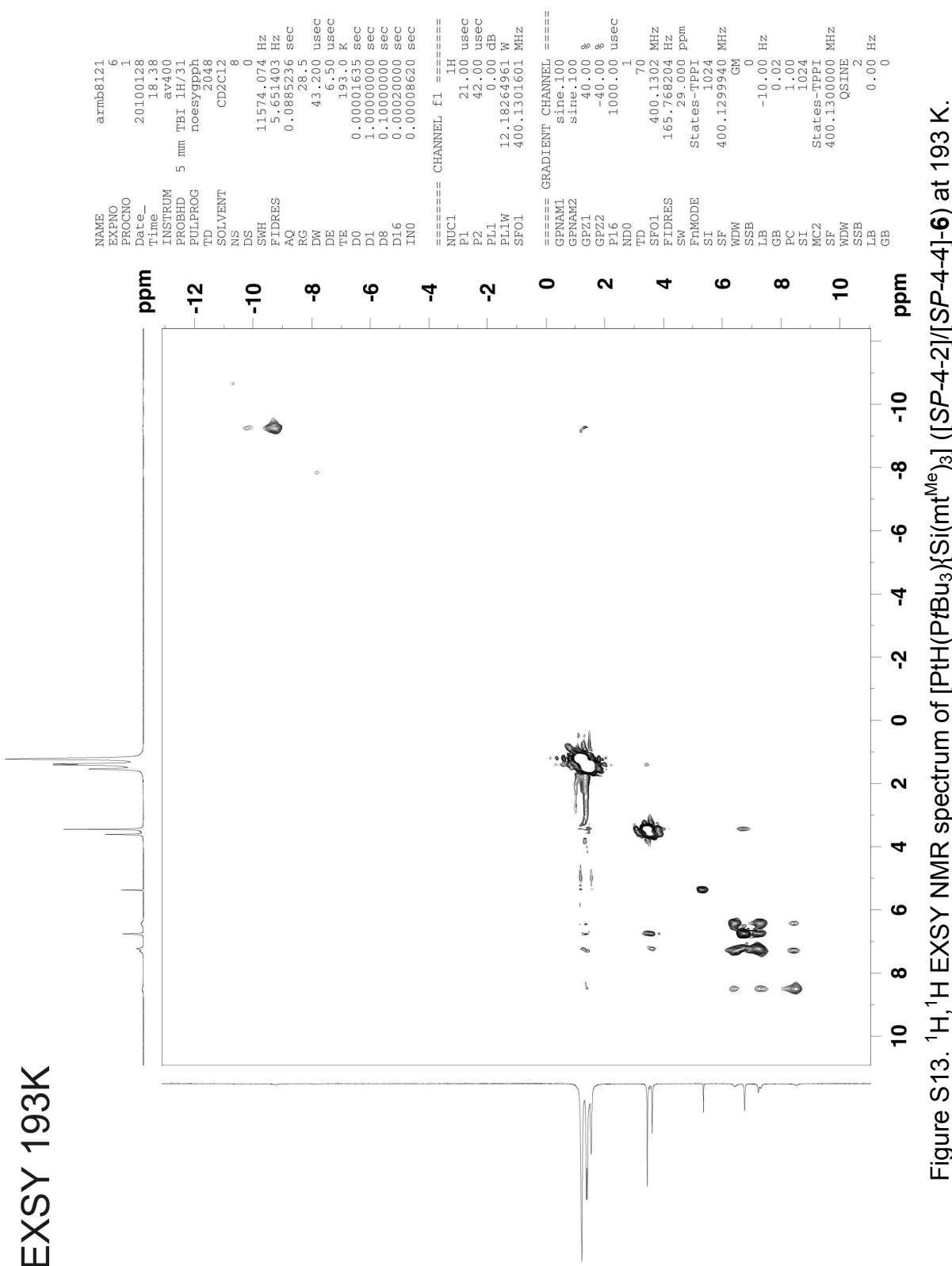


Figure S12.  $^1\text{H}$ ,  $^{195}\text{Pt}$  gHMQC NMR spectrum of  $[\text{Pth}(\text{PtBu}_3)\{\text{Si}(\text{mt}^{\text{Me}})_3\}]$  ( $[\text{SP-4-2}]/[\text{SP-4-4-6}]$ ) at RT (only the hydride region is shown).



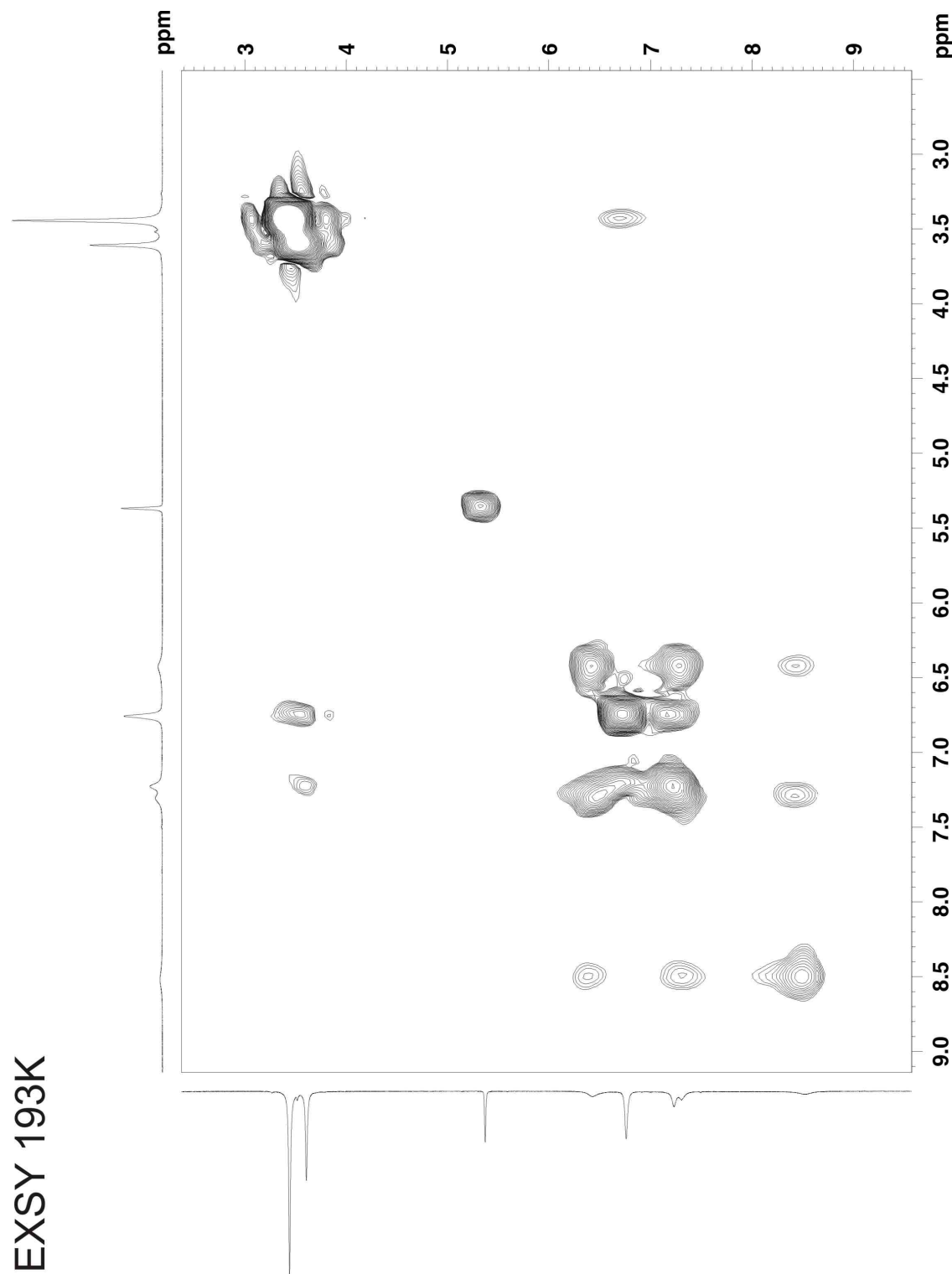


Figure S14.  $^1\text{H}$ ,  $^1\text{H}$  EXSY NMR spectrum of  $[\text{Pt}(\text{H}(\text{PtBu}_3)\{\text{Si}(\text{mt}^{\text{Me}})_3\} ([\text{SP-4-2}]/[\text{SP-4-4}]\text{-6})$  at 193 K (only the olefinic region is shown).

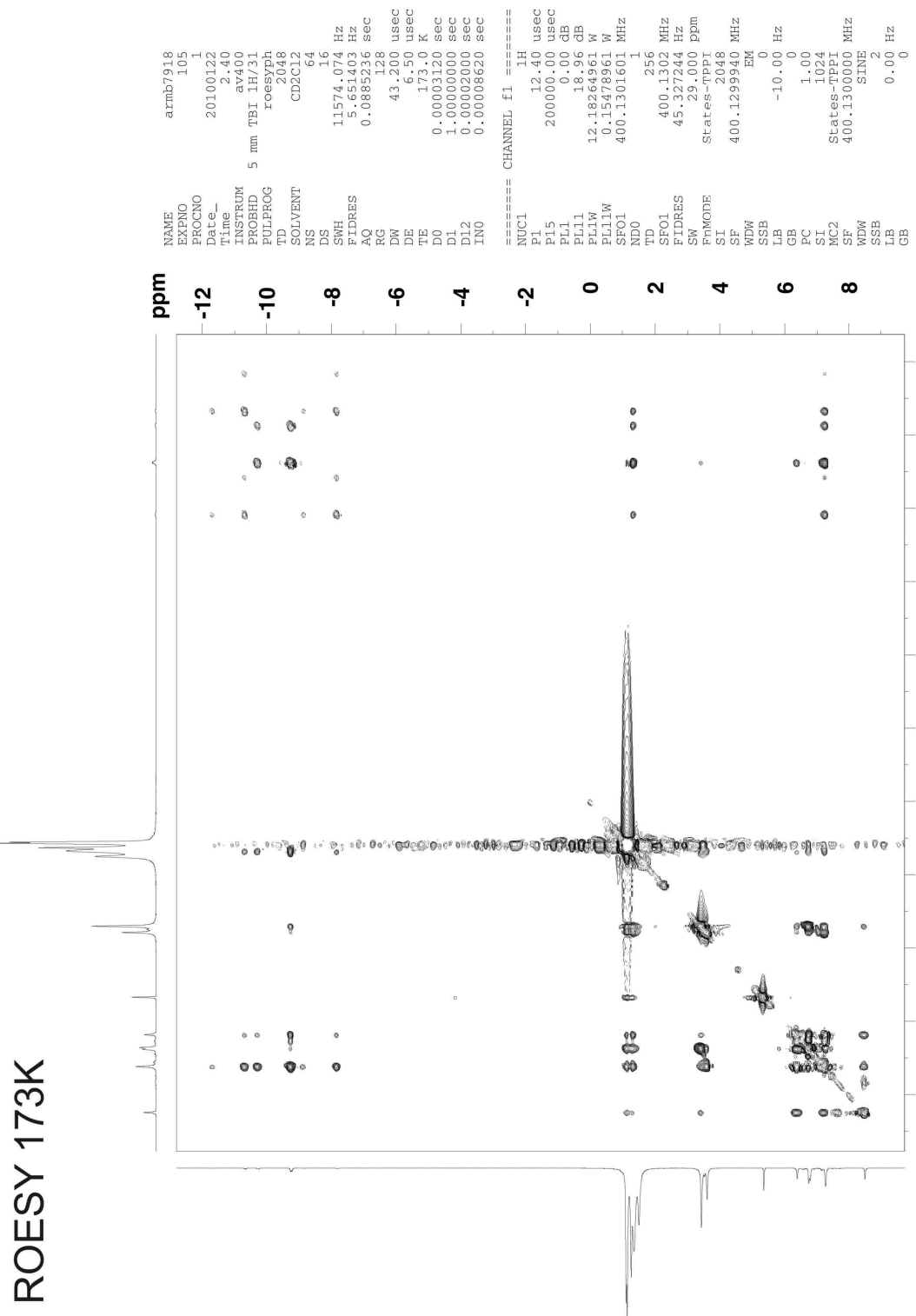


Figure S15.  $^1\text{H}$ , $^1\text{H}$  ROESY NMR spectrum of  $[\text{PtH}(\text{P}t\text{Bu}_3)\{\text{Si}(\text{mt}^{\text{Me}})_3\}][\text{SP-4-2}]/[\text{SP-4-6}]$  at 173 K.

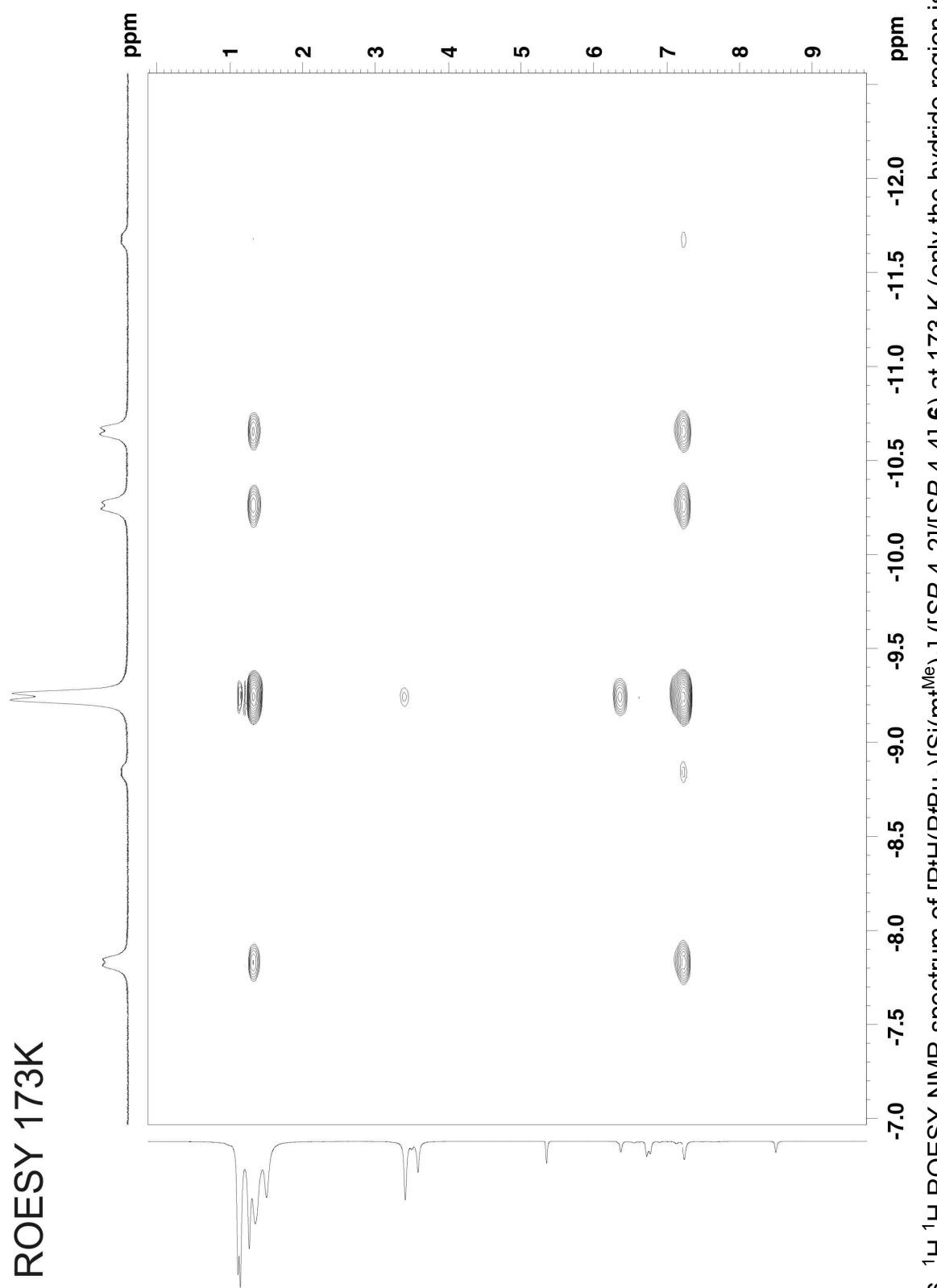


Figure S16.  $^1\text{H}$ ,  $^1\text{H}$  ROESY NMR spectrum of  $[\text{P}(\text{H}(\text{PtBu}_3)\{\text{Si}(\text{m}^1\text{Me})_3\}]$  ( $[\text{SP-4-2}]/[\text{SP-4-4}]$ -6) at 173 K (only the hydride region is shown).

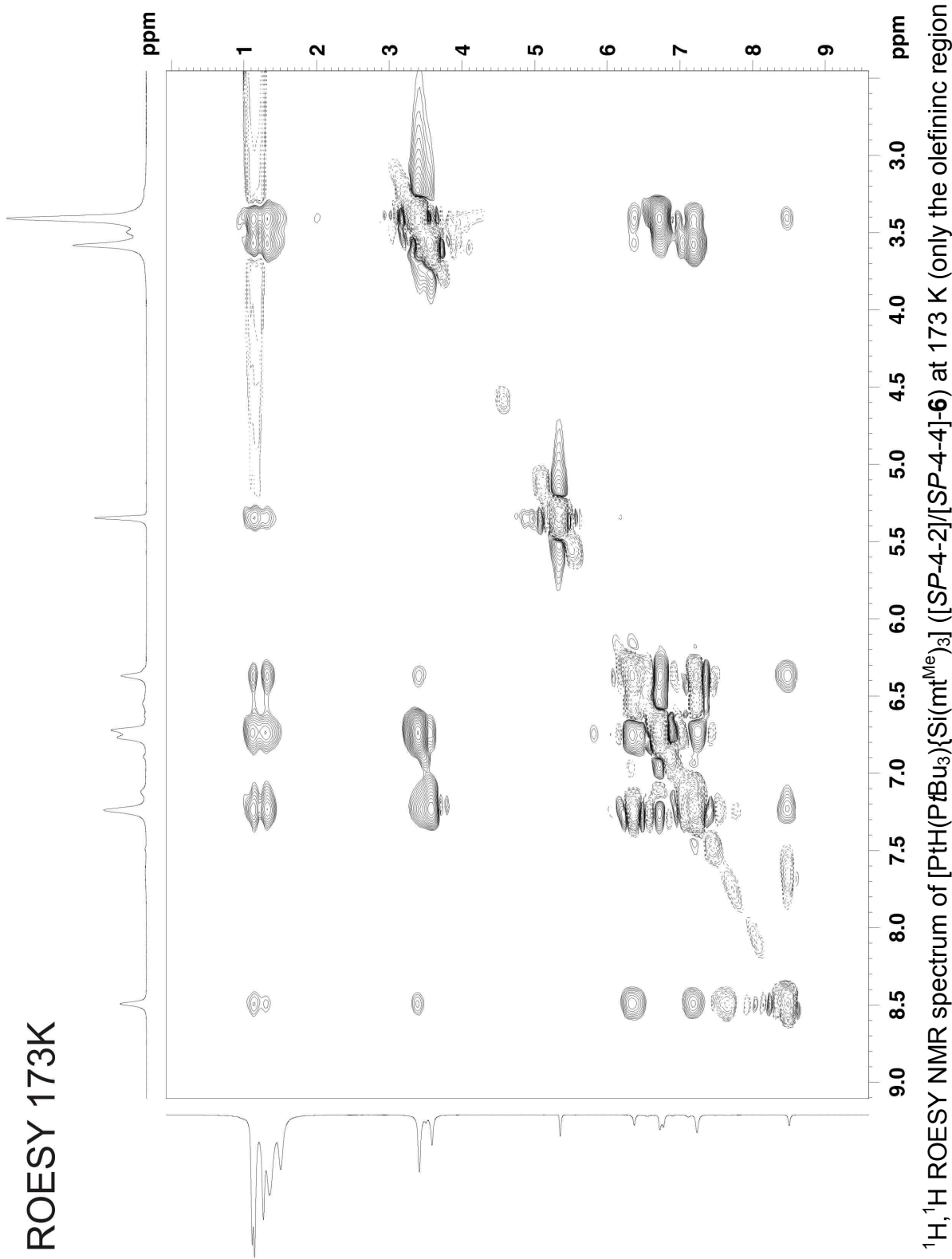


Figure S17.  $^1\text{H}$ , $^1\text{H}$  ROESY NMR spectrum of  $[\text{PtH}(\text{P}t\text{Bu}_3)\{\text{Si}(\text{mt}^{\text{Me}})_3\}](\text{SP-4-2})[\text{SP-4-4]-6}$ ) at 173 K (only the olefinic region is shown).

### References of the Supporting Information

- 
- [S1] P. Stilbs, *Prog. Nucl. Magn. Reson. Spectrosc.*, 1987, **23**, 1.
  - [S2] H. J. V. Tyrrell, K. R. Harris, *Diffusion in Liquids*, Butterworths, London, 1984.
  - [S3] (a) C. L. Yaws, *Chemical Properties Handbook*, McGraw-Hill, New York, 1999;  
(b) [www.knovel.com](http://www.knovel.com).
  - [S4] a) SHELXTL v6.12, Bruker AXS Inst. Inc., Madison, WI, USA (2000); b) G. M. Sheldrick, *Acta Crystallogr. Sect. A*, 2008, **64**, 112.
  - [S5] a) TURBOMOLE, V6.0, 2009, a development of University of Karlsruhe (TH) and Forschungszentrum Karlsruhe GmbH, 1989–2007, TURBOMOLE GmbH, since 2007, available from <http://www.turbomole.com>; b) R. Ahlrichs, M. Bär, M. Häser, H. Horn, C. Kölmel, *Chem. Phys. Lett.*, 1989, **162**, 165; c) O. Treutler, R. Ahlrichs, *J. Chem. Phys.*, 1995, **102**, 346; d) M. Sierka, A. Hogekamp, R. Ahlrichs, *J. Chem. Phys.*, 2003, **118**, 9136; e) R. Ahlrichs, *Phys. Chem. Chem. Phys.*, 2004, **6**, 5119.
  - [S6] a) J. C. Slater, *Phys. Rev.*, 1951, **81**, 385; b) S. H. Vosko, L. Wilk, M. Nusair, *Can. J. Phys.*, 1980, **58**, 1200; c) A. D. Becke, *Phys. Rev. A*, 1998, **38**, 3098; d) J. P. Perdew, *Phys. Rev. B*, 1986, **33**, 8822.
  - [S7] F. Weigend, R. Ahlrichs, *Phys. Chem. Chem. Phys.*, 2005, **7**, 3297.
  - [S8] F. Weigend, R. Ahlrichs, *Phys. Chem. Chem. Phys.*, 2006, **8**, 1057.
  - [S9] A. E. Reed, R. B. Weinstock, F. Weinhold, *J. Chem. Phys.*, 1985, **83**, 735.
  - [S10] C. Ehrhardt, R. Ahlrichs, *Theor. Chim. Acta*, 1985, **68**, 231.